A High-Performance Positive-Working Photosensitive Polyimide: Effects of Reactive End Groups on the Physical Properties of the Films

Myung-Sup Jung,[1,2] Won-Jae Joo,[1] Ohyun Kwon,[1] Byung H. Sohn,[1] Hee-Tae Jung[2]

[1]*Materials Center, Samsung Advanced Institute of Technology, Nongseo-dong, Giheung-gu, Yongin-si, Gyeonggi-do 446-712, Korea*
[2]*Department of Chemical and Biomolecular Engineering, Center for the Ultramicrochemical Process Systems, Korea Advanced Institute of Science and Technology, 373-1 Guseong-dong, Yuseong-gu, Daejeon 305-701, Korea*

Received 23 November 2005; accepted 1 February 2006
DOI 10.1002/app.24263
Published online in Wiley InterScience (www.interscience.wiley.com).

ABSTRACT: To investigate the effects of reactive end-cappers on the performance of PI precursors and the resulting polyimide (PI) films, poly(amic acid)s (PAAs) as a base polymer of the positive-working photosensitive polyimides (PSPIs) were synthesized via ring-opening polymerization of 4,4′-oxydiphthalic anhydride and 4,4′-oxydianiline with four different reactive end-cappers [maleic anhydride, citraconic anhydride, 2,3-dimethylmaleic anhydride (DMA), and 5-norbornene-2,3-dicarboxylic anhydride (NDA)]. During imidization of these end-capped PAAs to form the corresponding PI films, chain extension and crosslinking reactions of the respective end groups occurred, resulting in an improvement in the mechanical and thermal properties despite the low molecular weight of the precursors. However, the UV transmittance at ~365 nm, an important property of PSPIs for thick-film applications, such as stress buffer layers, was strongly influenced by the type of end-capper used. These behaviors were understood in terms of the optimized geometries and the simulated UV–vis spectra of modeled end groups determined from density functional theory calculations. © 2006 Wiley Periodicals, Inc. J Appl Polym Sci 102: 2180–2188, 2006

Key words: photosensitive polyimide; photolithography; reactive end-capper

INTRODUCTION

Photosensitive polyimides (PSPIs) have attracted much attention in recent years because their use in the fabrication of microelectronics can reduce the number of processing steps required to obtain the desired photolithographic pattern.[1] The widest application of PSPIs is as the stress buffer layer of semiconductor applied after chip passivation.[2] For such application, the PSPIs must exhibit good mechanical and thermal properties to protect the bare chip from the stresses induced by fillers in the molding compounds, and by the thermal mismatches that occur between the passivation layer and the molding compound.[2–4]

In particular, positive-working PSPIs have recently replaced conventional polyimides (PIs) as buffer coatings in semiconductor packaging. The use of positive-working PSPIs[5–7] rather than negative-working PSPIs[8,9] is preferred in lithography because of their many advantages, such as lower sensitivity to dust particles, better suited shapes for the pattern profiles in multilayer systems, developability with alkaline aqueous solutions, and reduced impact on the environment.[10] However, it is difficult to obtain good mechanical properties in PI films prepared from positive-working PSPIs, since the photosensitive group of the PI precursor and the additives used in the precursor composition strongly affect the morphological structure of the PI precursor in the condensed state as well as the imidization kinetics, which invariably leads to different structures and properties in the resulting PI films.[11,12] Another important requirement for PI precursors is high transmittance in the *i*-line (365 nm), which is a critical factor for thick-film applications such as stress buffer layers. To obtain high-resolution patterns with relatively thick films (over ~10 μm before curing), the PI precursors must be transparent at 365 nm. Thus, the design of a new PI precursor for positive-working PSPIs that satisfies all the above requirements is essential if PI films are to be used in practical applications such as stress buffer layers.

Here, we show that the PI films imidized from the end-capped PAAs are found to be very effective in the improvement of the performance of PIs. Four different reactive end-cappers [maleic anhydride (MA), citraconic anhydride (CA), 2,3-dimethylmaleic anhydride (DMA), and 5-norbornene-2,3-dicarboxylic anhydride

Correspondence to: H.-T. Jung (heetae@kaist.ac.kr).
Contract grant sponsor: Korea Ministry of Commerce, Industry and Energy.
Contract grant sponsor: Brain Korea 21 Program.

© 2006 Wiley Periodicals, Inc.

(NDA)] were introduced into the ends of the PI precursor chains. The use of these reactive end-cappers significantly improved the mechanical and thermal properties of the resulting PI films. However, the UV transmittance of these end-capped PAAs, which is an important property of PSPIs for thick-film applications, depended significantly on the type of end-capper used. Density functional theory (DFT) calculations verified that this dependence is due to the π-conjugation effect observed within the ring-opened structures of the end-cappers.

EXPERIMENTAL

Materials

Anhydrous *N*-methyl-2-pyrrolidinone (NMP) was obtained from ISP Technologies (Wayne, NJ) and dehydrated with 4 Å molecular sieves prior to use. 4,4′-Oxydiphthalic anhydride (ODPA) was obtained from Shanghai Research Institute (China) and used after vacuum drying at 130°C for 5 h. 4,4′-Oxydianiline (ODA) was obtained from Wakayama Seika Kogyo Co. (Japan) and used as-received. 5-Norbornene-2,3-dicarboxylic anhydride (NDA, Tokyo Kasei Kogyo Co., Japan), maleic anhydride (MA, Aldrich), and 2,3-dimethylmaleic anhydride (DMA, Aldrich) were purified by recrystallization from benzene. Citraconic anhydride (CA, Aldrich) was used as-received.

Synthesis of end-capped PAAs

The synthetic procedure of the end-capped PAAs is illustrated in Scheme 1. In a 250-mL round-bottom flask, 10.01 g (0.05 mol) of ODA was dissolved in 60 mL of NMP. While keeping the flask at 0–5°C, 13.18 g (0.0425 mol) of ODPA was slowly added to the flask with stirring. The resulting solution was stirred for an additional 2 h, and then 0.015 mol of end-capper (MA, CA, DMA, and NDA) was slowly added and stirred at 0–5°C for a further 16 h. The notations used for the end-capped poly(amic acid) (PAA) based on ODPA and ODA are as in the following example: NDA30-PAA represents a PAA with a 0.3*M* ratio of NDA to ODA.

Preparation of PI films

The PSPI precursor was spin-coated on a Si wafer, and then heat treated on a hot plate at 80°C for 10 min. Thermal imidization was then carried out in an electronic furnace (KDF S-80) with a multi-step process: successive heating at 5°C/min up to 200°C, 200°C for 60 min, 4°C/min up to 310°C, and 310°C for 60 min. The cured film was peeled from the wafer by soaking it in an aqueous solution of hydrofluoric acid (2% w/w) for 30 min. The notations of the end-capped PIs are as in the following example: NDA30-PI represents a PI imidized (finally at 310°C) from PAA with a 0.3*M* ratio of NDA to ODA.

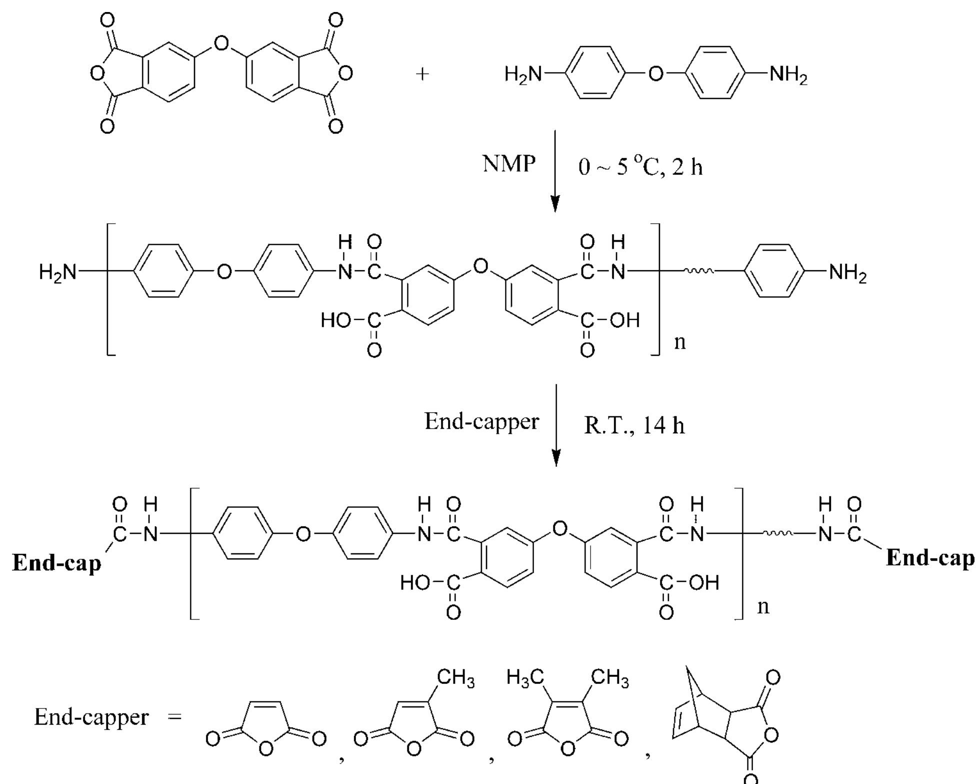

Scheme 1 Synthesis of reactive end-capped poly(amic acid)s.

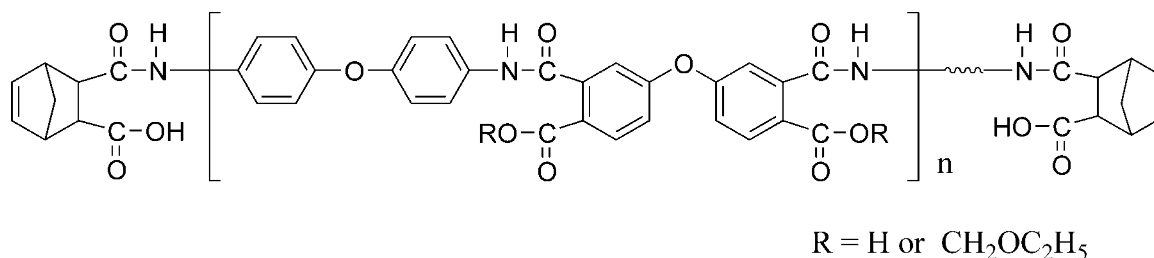

Scheme 2 The structure of norbornene end-capped poly(amic acid ethoxymethyl ester).

Measurements

The chemical structures of the reactive end groups of the PAAs were identified by ^{1}H-NMR with a Bruker Avance 300 spectrometer. Dimethyl sulfoxide-d_6 was used as the solvent. Gel permeation chromatography (GPC, Polymer Laboratory PL-GPC210) for molecular weight determination of the PI precursors was performed at 40°C in *N*,*N*-dimethylformamide (DMF) at a flow rate of 1 mL/min. The weight–average and number–average molecular weights were calculated with respect to polystyrene standards. The UV transmittance spectra were obtained on a JASCO V-560 UV–vis spectrophotometer. The mechanical properties of the PI films were measured using a Universal Testing Machine (UTM, Shimadzu AGS-G) in the tensile test mode at a rate of 3 mm/min. Test pieces with a width of 1 cm and a length of 8 cm were cut from the peeled PI films, and their film thicknesses were measured with a digital micrometer (Mitutoyo). The glass-transition temperature (T_g) and thermal expansion coefficient (TEC) were measured using a thermo mechanical analyzer (TA instruments TMA 2980) at a heating rate of 10°C/min under a nitrogen atmosphere. The pattern profiles of the corresponding PI films were obtained with a scanning electron microscope (SEM, JEOL JSM-5600).

Preparation of PSPI precursor composition and its lithographic evaluation

Appropriately, 1.2 g of the NDA30-poly(amic acid ethoxymethyl ester) (NDA30-PAAE), 1.8 g of the DMA30-PAA, and 0.45 g of a photo acid generator (PAG) were dissolved in 7 g of NMP to provide a PSPI precursor composition. NDA30-PAAE was synthesized as described in our previous report.[13] A protection ratio value of $\sim$ 60% for the ethoxymethyl group was optimized on the basis of dissolution rate studies. The structure of norbornene end-capped PAAE is shown in Scheme 2. Diphenyliodonium 5-hydroxynaphthalene-1-sulfonate (DINS) was synthesized and used as a PAG.[14] The resulting solution was spin-coated on Si wafers and prebaked at 90°C for 4 min. A photomask was then vacuum-pressed against the coated silicon wafer, and this was irradiated with the filtered UV light of wavelength 365 nm using a high-pressure mercury lamp (ORIEL Instruments). Next, the silicon wafer was postexposure baked at 130°C for 3 min, then developed with 2.38% (w/v) tetramethylammonium hydroxide (TMAH) solution for 4 min, and finally washed with distilled water to give a clear-patterned film. The thickness of the patterned PSPI film was 12 μm after development.

Molecular calculations

To understand the UV transparencies of the PAAs with various end-cappers, quantum-mechanical calculations were carried out. The geometries of the model end groups were optimized at the B3LYP/6-31G** level[15] in the DFT formalism,[16,17] which has been successfully used to obtain accurate molecular geometries compared to experimental data.[16,18] The ZINDO/S method[19] was applied to simulate UV–vis spectra based on DFT optimized geometries. The active space included the 10 highest occupied and 10 lowest unoccupied molecular orbitals for single excitations. It is well known that the ZINDO/S model exhibits good accuracy for the prediction of electronic excitations for organic π-conjugated systems.[19] All calculations were carried out using the Gaussian 98 program.[20]

RESULTS AND DISSCUSSION

Synthesis and characterization of PI precursors with reactive end-cappers

PAAs end-capped with maleic acid and norbornene groups were synthesized to improve the performance of PI films. The resulting bismaleimide and bisnadimide thermosetting PI precursors, which are low-molecular-weight telechelic oligomers end-capped with reactive functionalities, have been used as resins in high-temperature (> 200°C) applications for electronic devices. These oligomers were synthesized via the conventional reaction between an aromatic dianhydride and an aromatic diamine in the presence of a monofunctional end-capper (Scheme 1). The end-cappers carry a functional group susceptible to polymerization, copolymerization or crosslinking,[21] and can be polymerized under thermal activation without forming any volatile residues.

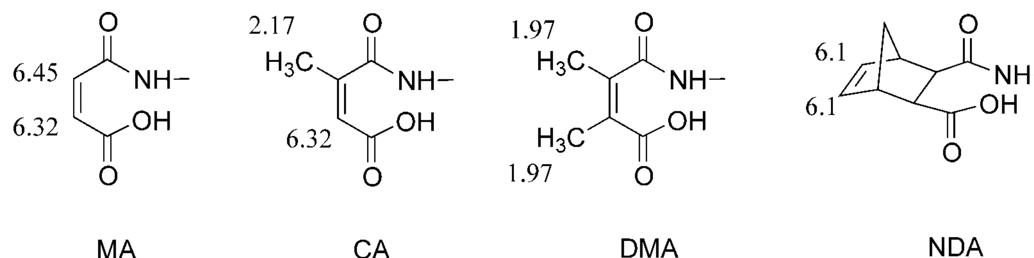

Figure 1 Ring-opened structures of reactive end-groups in PAA and their peaks (ppm) in ^{1}H-NMR spectra.

In this study, PAA was used as the backbone structure of the end-capped PI precursors, although other PI precursors, including poly(amic ester),[6,22] soluble PI,[5,23] and polyisoimide,[24] are also feasible as base polymers for positive-working PSPIs. For thick film applications such as stress buffer layers, however, the soluble PI and polyisoimide are not suitable as base polymers because of their strong absorbance at 365 nm. In the case of poly(amic ester), the resulting PI films have critical limitations in their mechanical properties due to the ester groups.[11] To improve the performance of the PSPI precursors and their imidized PI films, we designed PAAs with the four following end-cappers: MA, CA, DMA, and NDA (Scheme 1). These end-cappers were chosen on the basis of the prediction that PI films damaged by the photosensitive group or additives can be reinforced through chain extension and crosslinking reactions during thermal imidization. The bismaleimide and bisnadimide precursors were prepared from the ring-opening polymerization of ODPA and ODA in the presence of each reactive end-capper. The molar ratio of monomers was adjusted as ODPA : ODA : end-capper = $(2 - x)/2 : 2 : x$, where x represents the molar ratio of the end-capper.

The introduction of reactive end groups into the ends of PAAs was confirmed by ^{1}H-NMR spectroscopy (Fig. 1). The peaks associated with the CH=CH bond of the ring-opened structure of the MA end-capped PAA were observed at 6.45 and 6.32 ppm. Similarly, the peak due to the methyl group in the ring-opened structure of CA (2.17 ppm), the two methyl groups in the ring-opened structure of DMA (1.97 ppm), and the CH=CH bond in the ring-opened structure of NDA (6.1 ppm) all confirmed their introduction to the ends of the PI precursor chains. The number–average molecular weights of each end-capped PAA were distributed in the range of 1800–2100. The molecular weights of the PAAs were significantly lowered due to a stoichiometric imbalance between ODPA and ODA following the introduction of the end-cappers (Table I). The use of such low-molecular-weight PI precursors simplifies the purification process such as the filtration of PSPI precursor solutions to remove impurities or particles. Also, a moderate viscosity with high solid content can be easily realized without loss of the desired mechanical properties required for thick films applications such as stress buffer and dielectric layers in semiconductor packaging. This moderate viscosity with high solid content offers an effective, single step spin-coating process for the fabrication of films with a thickness over 10 μm.

TABLE I
Molecular Weight of End-Capped PAAs

	M_n	M_w	PDI (M_w/M_n)
NDA30	2,140	3,190	1.49
DMA30	1,950	2,790	1.43
CA30	1,810	2,550	1.41
MA30	1,850	2,660	1.44

Thermal and mechanical properties of PI films

Figure 2 shows the TMA curves of the PI films imidized from each end-capped PAA at 310°C. The T_g of each end-capped PAA is in the range of 230–270 °C, which is relatively high considering the low molecular weight of the corresponding precursors, but comparatively low with respect to conventional PIs. This is due to the low molecular weight of the PAAs used, although the cross-linked structure was formed by thermal reaction between reactive end-cappers.

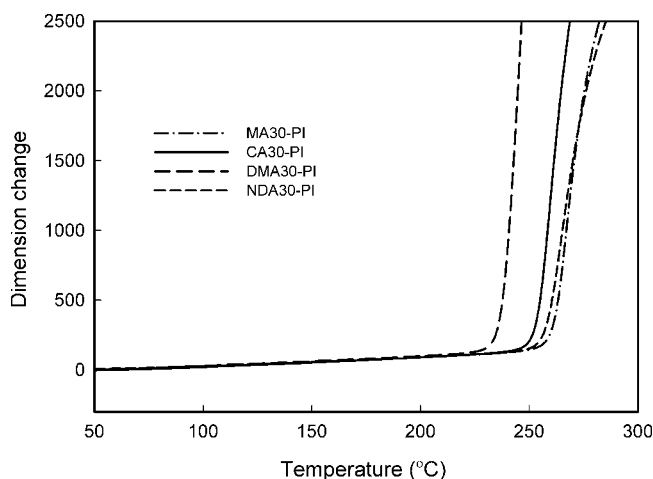

Figure 2 TMA graphs of PI films imidized from various PAAs.

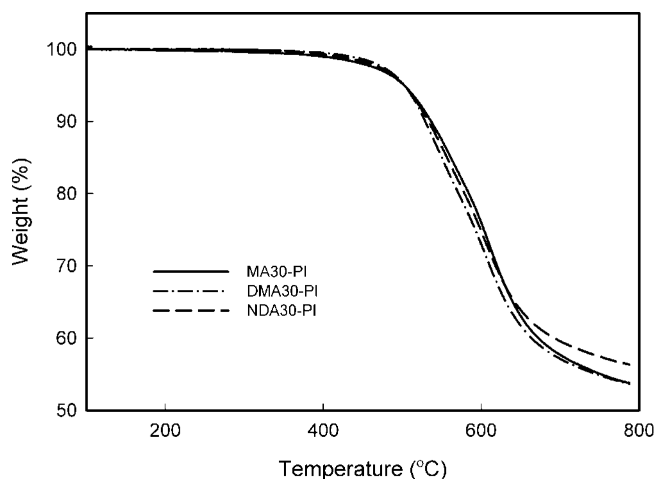

Figure 3 TGA graphs of PI films imidized from various PAAs.

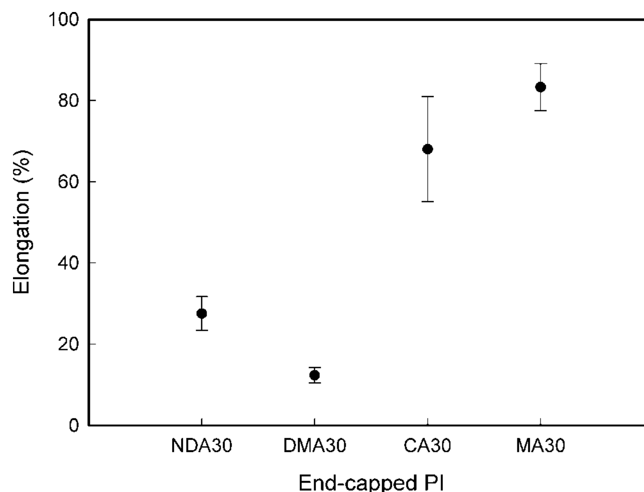

Figure 4 Elongation properties of PI films imidized from various PAAs.

Maleimide and norbornene have been widely used as typical reactive end-cappers in thermosetting PIs, and their respective curing reactions have been subject to numerous investigations.[21,25–29] These types of end-cappers differ from each other in the nature of the crosslinking mechanism. In the case of bismaleimide, the double bond of the maleimide end-capper forms free radicals, which react with each another to form a three-dimensional network during thermal imidization.[25] Crosslinked PI films cured from maleimide end-capped PAA exhibit relatively high T_g values (Fig. 2). However, the DMA30-PI imidized from DMA30-PAA exhibits a relatively low T_g compared to PI films containing other end-cappers. This indicates that the two methyl groups of DMA inhibit radical polymerization between the double bonds of the end groups for chain extension and crosslinking. Therefore, the DMA30-PI film has a lower crosslinking density than that of the MA30-PI and CA30-PI films. In the case of bisnadimide, several crosslinking mechanisms have been proposed based on model compound studies involving the copolymerization of maleimide end groups with free cyclopentadiene generated from the reverse Diels–Alder reaction of norbornene end groups at elevated temperature,[21,26,27] as well as from the direct copolymerization among norbornene end groups, maleimide end groups, and double cycloadducts formed by the Diels–Alder reaction between norbornene end groups and cyclopentadiene.[28,29] Regardless of the reaction mechanism, the pyrolysis of the nadimide termination seems to be a prerequisite for the initiation of the polymerization reaction. In Figure 2, the NDA30-PI film exhibits thermomechanical characteristics similar to those of the MA30-PI film.

Figure 3 shows the TGA curves of the PI films formed with various end-cappers. The thermal degradation behavior of the PI films was similar, and the 5% degradation temperature ($T_{d5\%}$) of all PI films was found to be about 500°C. This $T_{d5\%}$ value is somewhat low compared to that of conventional aromatic PIs, which is assumed to be due to the thermal degradation of the aliphatic crosslinking structure formed by the reactive end-cappers.

The mechanical properties of the PI films were measured using a UTM. As shown in Figure 4, the PI films exhibit excellent elongation properties in spite of the low molecular weight of their precursors. The MA30-PI and C30-PI films exhibit excellent elongations at break of more than 70%. However, DMA30-PI and NDA30-PI show relatively low elongation properties compared with MA30-PI and CA30-PI. In the case of DMA30-PI, the two methyl groups of DMA inhibit both the chain extension and crosslinking reactions, corroborating the results obtained in the TMA analysis. In the case of NDA30-PI, it is likely that the reaction mechanism of

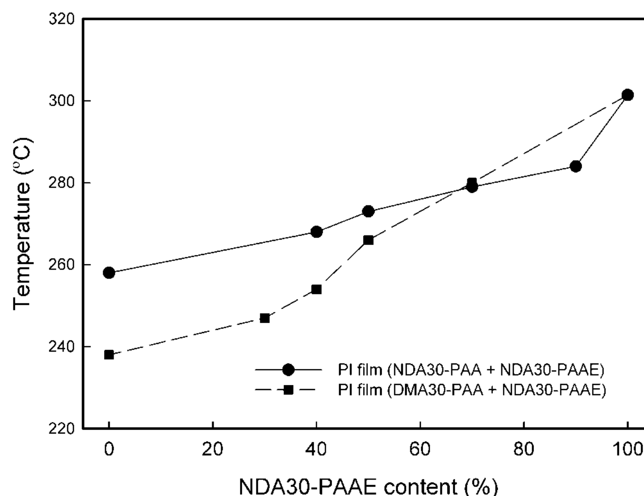

Figure 5 Effect of NDA30-PAAE content on the T_g of PI films prepared from blending mixtures of NDA30-PAAE and DMA30-PAA, and NDA30-PAAE and NDA30-PAA.

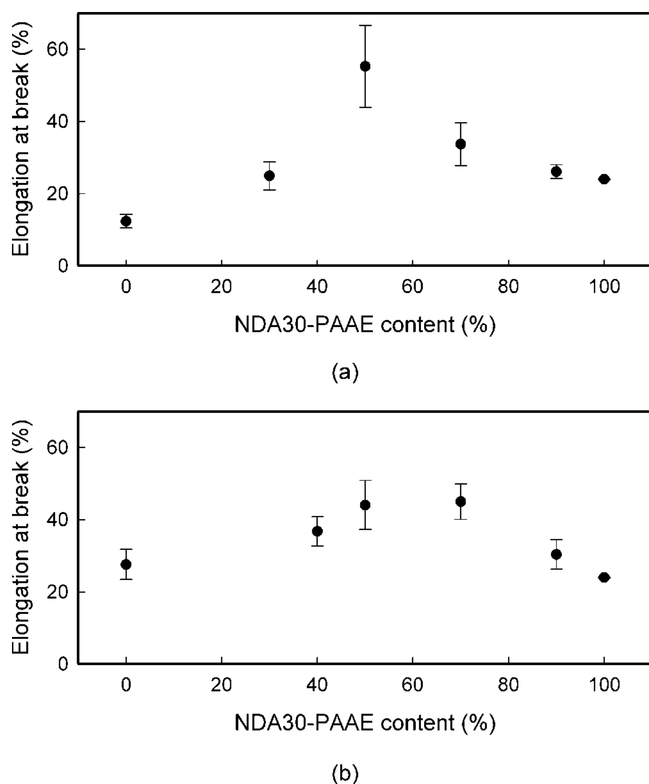

Figure 6 Effects of NDA30-PAAE content on the elongation properties of PI films prepared from (a) the blending mixture of NDA30-PAAE and DMA30-PAA, and (b) the blending mixture of NDA30-PAAE and NDA30-PAA.

norbornene groups is too complicated to understand the relatively low elongation properties.

Here, we describe a chemically amplified PSPI precursor system based on end-capped PI precursors and PAG. The solubility of these end-capped PAA in alkaline developer is too high to use as a base polymer for PSPI precursor system. Thus, to lower their high solubility in alkaline developer, the NDA30-PAAE as a polymeric dissolution inhibitor was blended with the end-capped PAA. Due to the complete insolubility of the NDA30-PAAE in alkaline developer, the solubility of the homogeneous blend was significantly decreased to a satisfactory level for the fabrication of high-resolution patterns with an optimized postexposure-bake process. Upon exposure to UV light, the PAG generates acid, which in combination with thermal energy, successively deprotects the acid-labile acetal groups of the NDA30-PAAE. The deprotected PI precursor and end-capped PAA in the exposed region can then be removed with a basic aqueous solution, and the unexposed region of the blend is converted to the desired PI pattern by thermal curing. Various amounts of NDA30-PAAE were blended with DMA30-PAA or NDA30-PAA, and the mechanical and thermal properties of the resulting PI films were measured to optimize the above properties.

As shown in Figure 5, the T_g of the PI films imidized from NDA30-PAAE is 301°C (see 100% of NDA30-PAAE content), which is a relatively high value compared with the PI films imidized from end-capped PAAs. This is due to the different imidization kinetics of poly(amic ester)s from PAA. Generally, the end groups of the bismaleimide precursor begin to polymerize at ~ 250°C, and the norbornene end groups of the bisnadimide precursor begin to polymerize or copolymerize at ~ 270°C via a reverse Diels–Alder reaction with the release of cyclopentadiene.[30] In the case of PAA, the majority of the amide-acid backbone was converted to imide groups below the polymerization temperature of the end-cappers during the curing process. The resulting imide backbone is stiff and rigid such that the chain mobility is lowered and the possibility of undergoing crosslinking reactions is limited. Therefore, the chain extension reaction is superior to crosslinking. On the other hand, the poly(amic ester) generally requires relatively higher temperature for the imidization than that required for PAA due to slow loss of the ester groups from the precursor.[31] Thus, the imidization reaction of the poly(amic ester) proceeds at around the same temperature as the polymerization of the end-cappers occurs. Therefore, a relatively flexible amide–acid backbone enables the formation of PI films with highly crosslinked structures. Hence, the T_g of the resulting PI film is higher than that of the PI film cured from end-capped PAA. For these reasons, the T_g of the PI film imidized from a blend mixture is increased in proportion to the NDA30-PAAE content (Fig. 5). These results clearly show that the crosslinking density is in proportion to the content of NDA30-PAAE.

The different imidization kinetics of poly(amic ester) also affects the mechanical properties of PI films. As shown in Figure 6(a, b), the elongation at break of the PI film varied significantly with the NDA30-PAAE content. In around 50% of NDA30-PAAE content, the PI films show the highest elongation properties. At this content, it is likely that corresponding crosslinking and chain extension reactions were adequately

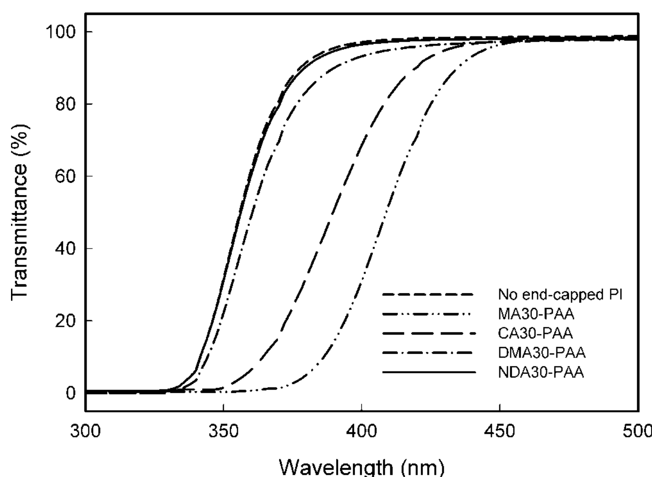

Figure 7 UV transmittance spectra of end-capped PAAs.

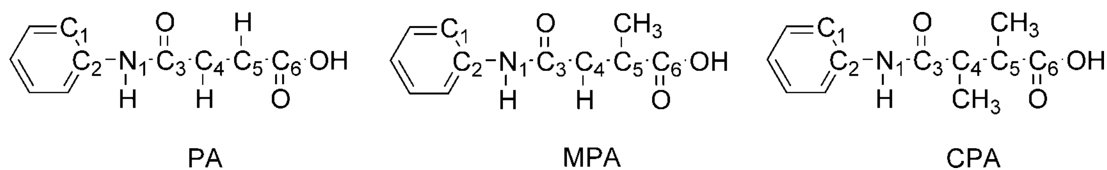

Scheme 3 The structures of model compounds.

controlled to obtain excellent mechanical properties. Above certain NDA30-PAAE content, the elongation at break was decreased due to an excessively crosslinked structure.

UV–vis spectra analysis and DFT calculation of model compounds

PSPIs have mostly been processed in mass production using *i*-line exposure tools. Hence, for thick-film applications such as buffer coatings, the base polymer must have high transparency at around 365 nm. Figure 7 shows the UV–vis spectra of various end-capped PAA films of thickness 10 μm. Although the ratio of end-cappers to whole polymer chains is very small, the end-cappers exert a strong influence on the absorbance of the PAA films. The PAA based on ODPA and ODA without end-cappers exhibits 69% of transmittance at 365 nm. The UV–vis spectrum of the NDA30-PAA film is very similar to that of the PAA, indicating that the introduction of NDA did not affect the absorbance of PAA. However, the introduction of MA type end-cappers (MA and CA) significantly changes the absorbance of PAA. By the ring-opening of MA, the UV absorbance of PAA shows a high bathochromic shift, due to the conjugation effect imparted by the end groups comprising two carbonyl groups and a double bond. The UV transmittances of MA30-PAA and CA30-PAA at ~ 365 nm were ~ 0% and 20%, respectively. As a result, the MA and CA end-cappers are not suitable for use as PSPI precursors. Although DMA is a MA type end-capper, the UV transmittance of DMA30-PAA was higher than that of the other MA end-cappers. This is likely due to the fact that conjugation of the end group is strongly inhibited by the two methyl groups. Similar behavior may occur in CA with one methyl group. The UV transmittance of CA30-PAA is only slightly less than that of MA30-PAA, due to the partially inhibited conjugation of the end groups.

To understand the different optical behaviors exhibited by the end-capped PAAs, the end group of each end-capped PAA was modeled as 3-phenylcarbamoyl-acrylic acid (PA), 2-methyl-3-phenylcarbamoyl-acrylic acid (MPA), and 2,3-dimethyl-3-phenylcarbamoyl-acrylic acid (DPA) (Scheme 3). The geometries of the modeled end groups were optimized at the B3LYP/6-31G** level[15] in the DFT formalism.[16,17] As summarized in Table II, the DFT-optimized geometrical parameters indicate that DPA shows a quite distorted geometry in the acrylic acid unit compared to PA and MPA. The dihedral angle of the acrylic unit in DPA is calculated to be 113.6° due to the steric hindrance of two methyl substituents, which leads to much less π-conjugation in the acrylic acid unit of DPA compared to that of PA (170.9°) and MPA (161.6°). This is also confirmed by the fact that the C_4C_5 bond distance is calculated to be 1.350 Å, which is larger than a typical C=C double bond (1.340 Å). UV–vis spectral simulations clearly show the different absorption pattern of the lowest excitation in DPA from that of PA and MPA, as seen in Figure 8. The lowest excitation of DPA occurs in the region of 230–270 nm (λ_{max} = 249 nm), where PA and MPA are transparent (calculated extinction coefficient 0). These results can be used to explain why the spectra of respective PAAs vary with different end-capper units.

TABLE II
Calculated Bond Distances (Å) and Dihedral Angles (°)

	PA	MPA	DPA
$r(C_2N_1)$	1.416	1.414	1.413
$r(N_1C_3)$	1.380	1.380	1.380
$r(C_3C_4)$	1.490	1.480	1.510
$r(C_4C_5)$	1.330	1.340	1.350
$r(C_5C_6)$	1.470	1.490	1.490
$\angle(C_1C_2N_1C_3)$	142.3	144.9	159.4
$\angle(C_2N_1C_3C_4)$	12.6	12.2	6.4
$\angle(N_1C_3C_4C_5)$	170.9	161.6	113.6
$\angle(C_3C_4C_5C_6)$	178.2	177.5	176.7

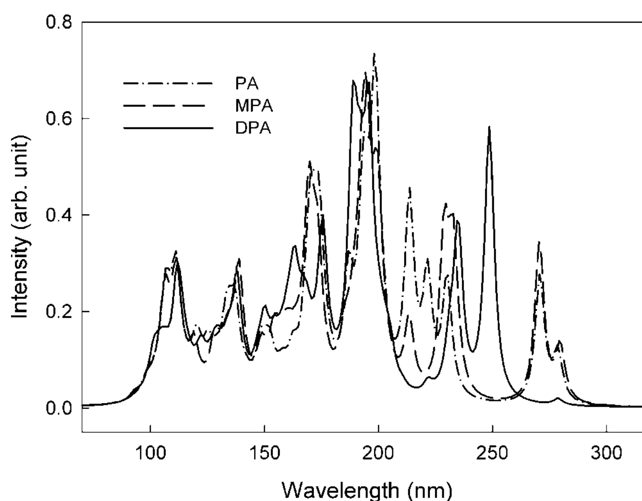

Figure 8 Simulated UV–vis spectra of modeled end groups.

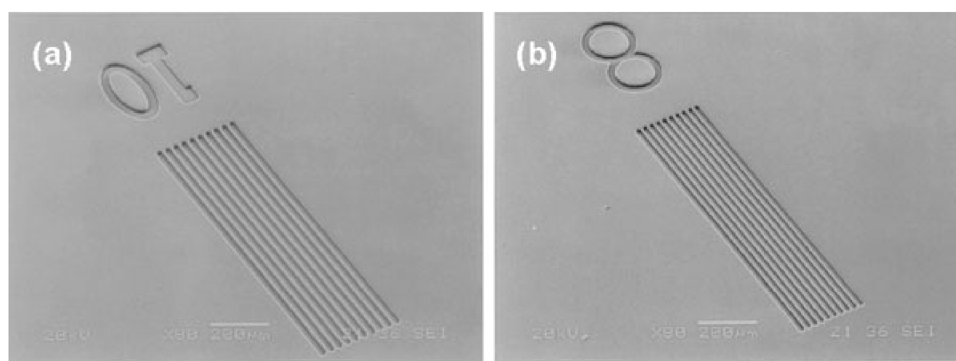

Figure 9 SEM images of PI precursor patterns after developing. (a) 10 μm L/S and (b) 8 μm L/S.

Photolithography

The PSPI precursor system was prepared by blending a mixture of NDA30-PAAE and DMA30-PAA with 13 wt % DINS. The UV–vis spectrum and photochemical reaction of the DINS were shown in our previous report.[13] The blending ratio was determined by considering the dissolution rate with respect to the developer, and the mechanical properties of the final blend. A detailed description concerning the formulation and lithographic evaluation of the PSPI precursor system is beyond the scope of this article and is thus not given in the present discussion. Figure 9 shows the SEM images of positive patterns produced from the PSPI precursor system after 1000 mJ/cm^2 of UV exposure at 365 nm, followed by the subsequent development the precursor film with TMAH aqueous solution. Figures 9(a) and 9(b) show the 10 μm line and space (L/S), and 8 μm L/S patterns (12 μm thickness) for the precursor film. Figure 10 shows the PI pattern obtained by thermal curing of the PI film at 310°C. Figures 10(a) and 10(b) show the corresponding 10 and 8 μm L/S patterns of the PI film, respectively. The patterned film thickness was reduced $\sim$ 29.3% compared to the precursor film after the thermal curing process. This film shrinkage is likely due to the imidization reaction, coupled with the loss of the ethoxymethyl groups in the polymer and the decomposition of the DINS. However, no distortion or deformation of the pattern was observed after thermal curing. Further studies into chemically amplified PSPIs bearing reactive end-capper groups, having high resolution and excellent physical properties, are in progress, particularly with respect to the practical use of thick films in applications such as buffer coatings in semiconductor manufacturing.

CONCLUSIONS

Although the molecular weights of the PI precursors (PAAs) were lowered by the introduction of the reactive end-cappers, the corresponding PI films exhibited excellent mechanical and thermal properties afforded by the chain extension and crosslinking reactions of the end-cappers. In addition, a UV–vis spectroscopic study of the effect of the end-cappers on the UV absorbance of PAA revealed that the UV absorbance of the PAAs varied markedly depending on the type of end-capper. Specifically, NDA had no effect on the UV absorbance of PAA, whereas the introduction of CA or MA end-cappers significantly affected the PAA absorbance around 365 nm due to the π-conjugation effect of their ring-opened structures. As a result, both CA and MA are considered unsuitable as end-cappers for the PI precursors of positive-type PSPIs, despite their role in improving the mechanical and thermal properties of the resulting PI film due to the excellent chain extension and crosslinking reactivity of the end groups. However,

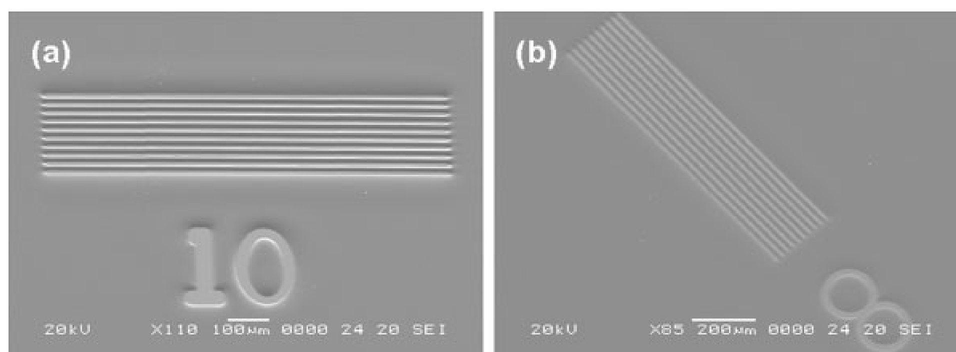

Figure 10 SEM images of PI patterns after thermal curing at 310°C. (a) 10 μm L/S and (b) 8 μm L/S.

although DMA is a MA type end-capper, the introduction of DMA caused a slight lowering in the UV transmittance of PAA, which is attributed to the strongly inhibited π-conjugation afforded by the two methyl groups of DMA. Consequently, the present results indicate that NDA and DMA can be utilized as the reactive end-capper units of low-molecular-weight PSPI precursors to improve the physical properties of the resulting imidized PI films.

References

1. Horie, K.; Yamashita, T. Photosensitive Polyimides, Fundamentals and Applications; Technomic: Lancaster, 1995.
2. Culver, R. Solid State Technol 1997, 40, 151.
3. Prack, E.; Tran, Z.; Franklin, C.; Tanner, S.; Murray, D. O. Adv Electron Packag 1997, 1, 1141.
4. Flack, W. W.; Flores, G. E.; Christensen, L.; Newman, G. Proc SPIE 1996, 2726, 169.
5. Hsu, S. L.-C.; Lee, P.; King, J. S.; Jeng, J. L. J Appl Polym Sci 2002, 86, 352.
6. Hsu, S. L.-C.; Lee, P.; King, J. S.; Jeng, J. L. J Appl Polym Sci 2003, 90, 2293.
7. Ho, B.-C.; Chen, J.-H.; Perng, W. C.; Lin, C. L.; Chen, L. M. J Appl Polym Sci 1998, 67, 1313.
8. Jin, Q.; Yamashita, T.; Horie, K. J Polym Sci Part A: Polym Chem 1994, 32, 503.
9. Chen, H.; Yin, J. J Polym Sci Part A: Polym Chem 2004, 42, 1735.
10. Ahne, H.; Leuschner, R.; Rubner, R. Polym Adv Technol 1993, 4, 217.
11. Ree, M. H.; Nunes, T. L.; Chen, K. J. R. J Polym Sci Part B: Polym Phys 1995, 33, 453.
12. Yoneda, Y.; Mizutani, D.; Ishiduki, Y.; Yokouchi, K. J Photopolym Sci Technol 1996, 9, 323.
13. Jung, M. S.; Lee, S. K.; Hyeon-Lee, J.; Park, M. K.; Jung, H. T. J Polym Sci Part A: Polym Chem 2005, 43, 5520.
14. Jung, M. S.; Seo, S. J. (to Samsung Electronics Co.). U.S. Pat 6,541,178 (2003).
15. Becke, A. D. J Chem Phys 1993, 98, 5648.
16. Koch, W.; Holthausen, M. C. A Chemist's Guide to Density Functional Theory; Wiley: New York, 2000.
17. Parr, R. G.; Yang, W. Density Functional Theory of Atoms and Molecules; Oxford University Press: Oxford, 1989.
18. Cramer, C. J. Essentials of Computational Chemistry: Theories and Models; Wiley: New York, 2001.
19. Bacon, A. D.; Zerner, M. C. Theor Chim Acta 1979, 53, 21.
20. Frisch, M. J.; Trucks, G. W.; Schlegel, H. B.; Scuseria, G. E.; Robb, M. A.; Cheeseman, J. R.; Zakrzewski, V. G. et al. Gaussian 98 Release Notes Rev. A. 9; Gaussian: Pittsburgh, PA, 1998.
21. Bertholio, F. B.; Mison, P.; Pascal, T.; Sillion, B. High Perform Polym 1993, 5, 47.
22. Kubota, S.; Yamawaki, Y.; Moriwaki, T.; Eto, S. Polym Eng Sci 1989, 29, 950.
23. Omote, T.; Mochizuki, H.; Koseki, K.; Yamaoka, T. Macromolecules 1990, 23, 4796.
24. Seino, H.; Haba, O.; Ueda, M.; Mochizuki, A. Polymer 1999, 40, 551.
25. Torrecillas, R.; Regnier, N.; Mortaigne, B. Polym Degrad Stab 1996, 51, 307.
26. Chisholm, M. S.; Dewar, W. S.; Smith, D. M. J Mater Chem 1995, 5, 947.
27. Hu, A. J.; Hao, J. Y.; Yang, S. Y. Macromolecules 1999, 32, 8046.
28. Wong, A. C.; Ritchey, W. M. Macromolecules 1981, 14, 825.
29. Wong, A. C.; Garroway, A. N.; Ritchey, W. M. Macromolecules 1981, 14, 832.
30. Stenchenberger, H. D. In Polyimides; Wilson, D., Stenchenberger, H. D., Hergenrother, P. M., Eds.; Blackie: London, 1993; Chapter 4.
31. Coburn, J. C.; Pottiger, M. T. In Polyimides: Fundamentals and Applications; Ghosh, M. K., Mittal, K. L., Eds.; Marcel Dekker: New York, 1996; Chapter 8.